JOURNAL OF GEOPHYSICAL RESEARCH: EARTH SURFACE, VOL. 118, 2354–2364, doi:10.1002/2013JF002742, 2013

Structural and environmental controls on Antarctic ice shelf rift propagation inferred from satellite monitoring

C. C. Walker,[1] J. N. Bassis,[1] H. A. Fricker,[2] and R. J. Czerwinski[1]

Received 28 January 2013; revised 25 September 2013; accepted 12 October 2013; published 13 November 2013.

[1] Iceberg calving from ice shelves accounts for nearly half of the mass loss from the Antarctic Ice Sheet, yet our understanding of this process is limited. The precursor to iceberg calving is large through-cutting fractures, called "rifts," that can propagate for decades after they have initiated until they become iceberg detachment boundaries. To improve our knowledge of rift propagation, we monitored the lengths of 78 rifts in 13 Antarctic ice shelves using satellite imagery from the Moderate Resolution Imaging Spectroradiometer and Multiangle Imaging Spectroradiometer between 2002 and 2012. This data set allowed us to monitor trends in rift propagation over the past decade and test if variation in trends is controlled by variable environmental forcings. We found that 43 of the 78 rifts were dormant, i.e., propagated less than 500 m over the observational interval. We found only seven rifts propagated continuously throughout the decade. An additional eight rifts propagated for at least 2 years prior to arresting and remaining dormant for the rest of the decade, and 13 rifts exhibited isolated sudden bursts of propagation after 2 or more years of dormancy. Twelve of the fifteen active rifts were initiated at the ice shelf fronts, suggesting that front-initiated rifts are more active than across-flow rifts. Although we did not find a link between the observed variability in rift propagation rate and changes in atmospheric temperature or sea ice concentration correlated with, we did find a statistically significant correlation between the arrival of tsunamis and propagation of front-initiated rifts in eight ice shelves. This suggests a connection between ice shelf rift propagation and mechanical ocean interaction that needs to be better understood.

Citation: Walker, C. C., J. N. Bassis, H. A. Fricker, and R. J. Czerwinski (2013), Structural and environmental controls on Antarctic ice shelf rift propagation inferred from satellite monitoring, *J. Geophys. Res. Earth Surf.*, *118*, 2354–2364, doi:10.1002/2013JF002742.

1. Introduction

[2] The Antarctic Ice Sheet is surrounded by platforms of floating ice called ice shelves, which are freely floating seaward extensions of the grounded ice sheet. Ice shelves play a crucial role in the overall mass balance of the Antarctic Ice Sheet because they are the sites of majority of the mass loss from the ice sheet to the Southern Ocean [*Rignot et al.*, 2008]. Although the mass lost from ice shelves does not directly contribute to sea level rise, observations show that thinning, retreat, or demise of ice shelves is linked to increased discharge of grounded ice [e.g., *De Angelis and Skvarca*, 2003; *Scambos et al.*, 2004; *Rignot et al.*, 2004; *Amundson and Truffer*, 2010; *Joughin et al.*, 2012; *Pritchard et al.*, 2012] , providing an indirect link between ice sheet stability and sea level rise.

[3] Mass loss from ice shelves occurs primarily through the processes of iceberg calving and basal melting [e.g., *Rignot et al.*, 2013]. Of these two processes, iceberg calving remains the least well understood. This is partly because calving events from Antarctic ice shelves occur sporadically with long (decades or longer) recurrence intervals between major calving events [*Holdsworth*, 1974; *Robinson and Haskell*, 1990; *Jacobs et al.*, 1986; *Lazzara et al.*, 1999; *Fricker et al.*, 2002]. Moreover, observations over the past decade show that ice shelves exhibit a spectrum of calving behaviors. For example, the Larsen A and B Ice Shelves abruptly disintegrated following a series of abnormally warm summers [e.g., *Scambos et al.*, 2003]. Not only were these disintegrations surprising in terms of their size but also in the short time over which they occurred [e.g., *Rott et al.*, 1996, 2002; *Scambos et al.*, 2003; *Rack and Rott*, 2004] and have been related to the abundance of surface melt associated with the approximately 3°C increase in temperature at the Antarctic Peninsula over the last half of the century [e.g., *Vaughan and Doake*, 1996; *Rott et al.*, 1998; *Scambos et al.*, 2000; *Fahnestock et al.*, 2002;

Additional supporting information may be found in the online version of this article.

[1]Department of Atmospheric Oceanic and Space Sciences, University of Michigan, Ann Arbor, Michigan, USA.

[2]Institute of Geophysics and Planetary Physics, Scripps Institution of Oceanography, La Jolla, California, USA.

Corresponding author: C. C. Walker, Department of Atmospheric Oceanic and Space Sciences, University of Michigan, Ann Arbor, MI 48109, USA. (catcolwa@umich.edu)

2169-9003/13/10.1002/2013JF002742

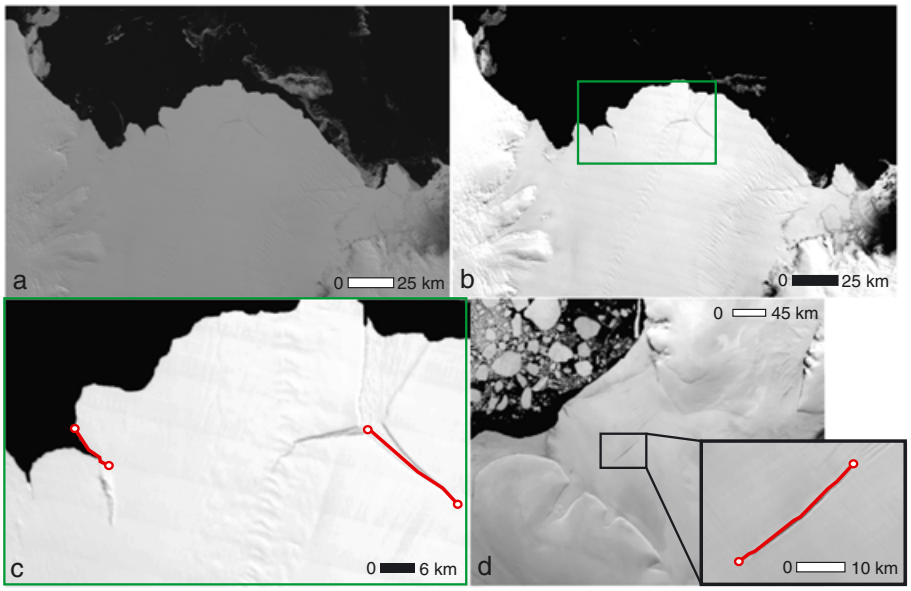

Figure 1. Image enhancement and methods of measuring rift length in Antarctic ice shelves for different rift orientations. (a) Raw MODIS image of the Amery Ice Shelf in East Antarctica from 11 February 2012. (b) Brightened and contrast-stretched version of same MODIS image. (c) Red circles denote beginning and end points for measuring rifts. Shown here is (left) a front-initiated rift and (right) a rift initiated from a triple junction. Red lines denote the measured length. (d) The Fimbul Ice Shelf in a contrast-enhanced MODIS image from February 2012. Inset: Red circles denote beginning and end points of measurement for a double-ended rift.

Steffen et al., 2008]. Recent observations on Larsen C Ice Shelf have also pointed to the potential role of wide basal crevasses in destabilizing the ice shelf [*Luckman et al.*, 2012; *McGrath et al.*, 2012]. On the other end of the spectrum, the larger ice shelves (Ross, Filchner-Ronne, and Amery Ice Shelves) are located in a colder climate, farther south than the Antarctic Peninsula, and have not experienced comparable surface warming nor are they currently showing any signs of imminent peninsular-style disintegration. Instead, these ice shelves exhibit a calving regime in which large tabular bergs detach with decades or even centuries between major calving events.

[4] In this study, we investigated the process that precedes iceberg calving, rift propagation, to determine possible driving environmental or structural mechanisms. Ice shelf rifts are fractures that have completely severed the ice thickness; alternately, crevasses are fractures that do not penetrate the entire ice shelf thickness. Rifts can propagate for decades before becoming the detachment boundaries of icebergs. Previous studies have reached different conclusions about the dominant forces driving rift propagation, with some studies suggesting that rift propagation is driven by the internal glaciological stress [*Joughin and MacAyeal*, 2005; *Bassis et al.*, 2005; *Benn et al.*, 2007; *Bassis et al.*, 2008; *Humbert and Steinhage*, 2011; *Bassis and Jacobs*, 2013] or by external effects like fatigue failure-inducing flexural wave propagation along the ice shelf [e.g., *Holdsworth*, 1977; *Lescarmontier et al.*, 2012] and stress accumulation and release by tide-induced currents in floating ice tongues [e.g., *Legresy et al.*, 2004]. Other studies have proposed that the timing of iceberg-calving events may be related to the arrival of pulses of ocean swell [*MacAyeal et al.*, 2006; *Bromirski et al.*, 2010; *Sergienko*, 2010] or even the arrival of tsunamis [*Brunt et al.*, 2011]. Previous studies have also noted that rifts tend to arrest at suture zones between ice streams [*Hulbe et al.*, 2010; *Glasser et al.*, 2009; *McGrath et al.*, 2012; *Luckman et al.*, 2012] with some speculation that marine ice filling these suture zones may form a barrier to rift propagation, producing a stabilizing effect on ice shelves [*Holland et al.*, 2010; *McGrath et al.*, 2012; *Jansen et al.*, 2013]. However, these studies have been based on a small sample of ice shelves, and it is not clear if these observations are universal or specific to individual ice shelves and glaciological settings.

[5] To improve these localized studies, we conducted an Antarctic-wide survey of ice shelf rift propagation rates for the decade 2002–2012 to test hypotheses about what drives rift propagation. We tracked 78 rifts in 13 ice shelves, each within 30 km of their respective calving fronts. The survey provides broad geographical coverage around the continent and also represents a variety of physical and environmental settings. Ice shelves ranged from the largest ice shelves (e.g., the Ross and Filchner-Ronne Ice Shelves) to smaller ice shelves (e.g., the Wilkins and West Ice Shelves). We used the resulting data set to analyze patterns of rift behavior around the continent.

2. Data and Methods

2.1. Satellite Imagery and Image Processing

[6] We used images from two different sensors on two separate spacecraft to maximize temporal sampling: the Multiangle Imaging Spectroradiometer (MISR; pixel size

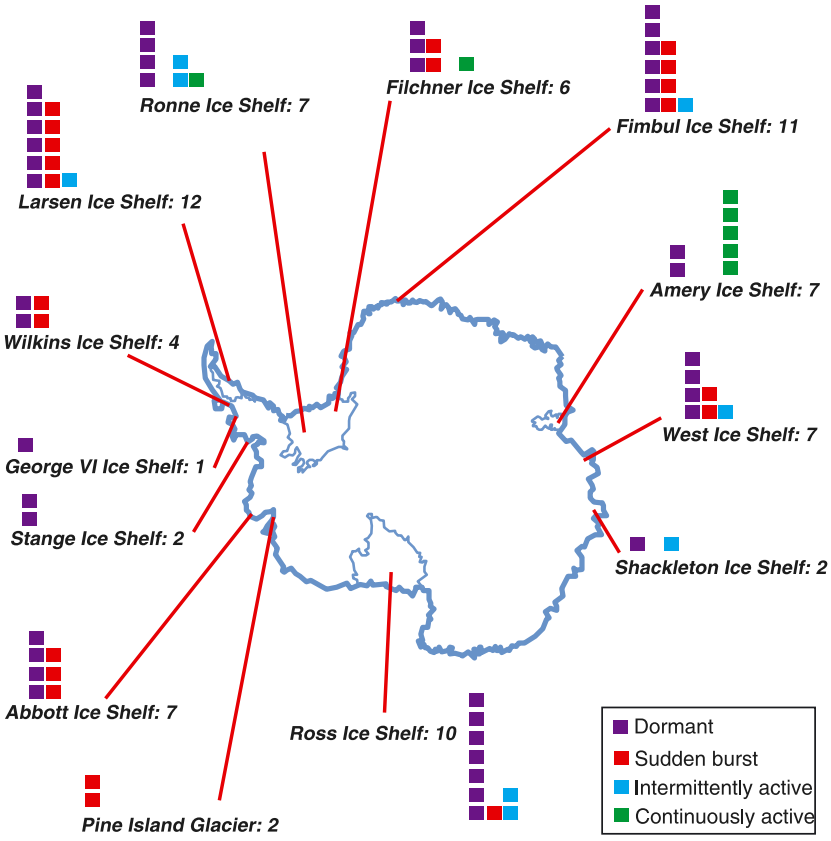

Figure 2. Antarctic ice shelf locations and categories of rift propagation observed. Each block denotes a rift, and the color of the block denotes the type of rift activity observed.

275 m) on NASA's Terra satellite and the Moderate Resolution Imaging Spectroradiometer (MODIS; pixel size 250 m) on both the Terra and Aqua satellites. We used visible channel MODIS imagery, which was available online from the National Snow and Ice Data Center (NSIDC) and required no additional processing [*Scambos et al.*, 1996]. For MISR, we generated false-color composites using the CF (camera C in the forward look direction), AN (the nadir camera), and CA (camera C in the aftward look direction) bands with the publicly available MISRView software. This allowed better detection of the rifts in the MISR images using this combination of bands from cameras looking at different angles; color acts as a proxy for angular reflectance variations which are related to surface texture and enhances the rifts [*Fricker et al.*, 2005]. For each MODIS and MISR image, we performed contrast stretching, toning, and brightening to enhance the visibility of the rifts and increase our ability to differentiate between the rift and ice shelf [*Fricker et al.*, 2005].

[7] Ice shelves included in this study were those with data with availability of (at least) monthly data over the decade, archived by the National Snow and Ice Data Center (NSIDC), and included rifts within 50 km of the ice shelf front. We searched through all available browse images of the ice shelf fronts between January 2002 and March 2012 to determine suitable images and selected only those that had an unobscured view of the ice front, i.e., only during cloud-free summer days (September to April). We analyzed about 60 images for each of the 78 rifts over the decade, for a total of approximately 5000 images.

2.2. Rift Length Measurement

[8] To estimate propagation rates for each rift, we first measured the length of each rift in every clear image (Figure 1). Because we only measured distances between two points on an image, we did not require any geolocation information. For "front-initiated" rifts (i.e., initiated from the calving front and propagating inward into the ice shelf), we measured the distance from the upstream rift wall edge to the rift tip. For rifts originating from an interior point in the ice shelf or a triple junction, we measured from tip-to-tip or from the center of the triple junction to the rift tips. We define the "rift tip" as the final point at which a rift pixel is discernible from the background; the true rift tip may extend much further than we can resolve in the MODIS and MISR images if the rift becomes narrower than a single pixel. Moreover, we are only able to discern the surface expression of the rift; therefore, we could not observe subsurface propagation or any portion of a rift tip possibly obscured by snow bridges. Our estimated precision in identifying the rift tip in MODIS and MISR imagery is approximately 1 pixel (~275 m for MISR and ~250 m for MODIS). Higher resolution Landsat imagery was used to spot-check propagating rifts to improve the visibility of rift tips and detect small crevasses in their vicinity. Because we rely on visible imagery, our study is limited to the Austral summer; Austral wintertime activity (if present) could only be estimated by rift length changes between autumn (March–April) and spring (September–October) images. We estimated rift propagation rates by dividing lengths by the number of days between measurements.

Table 1. Observations of Antarctic Ice Shelf Rift Propagation 2002–2012

Name	Origin Location	Event Description	Start Date	End Date	Length Change (km)	Crevasse Rate (m/day)	Propagation Visible Field?	Notes
				Fimbul				
N1	FI	Propagation to front, iceberg calving	September 2009	October 2009	5	80	No	Iceberg (km^2)
J2	FI	Split into TJ prior to 2002	–	–	–	–	Yes	
J2a	TJ (J2)	Propagation	September 2002	December 2002	6	3.8	Yes	
		Propagation to front, iceberg calving	March 2007	April 2007	2	110	Yes	Offshoot rift initiated after calving
J2b	TJ (J2)	Propagation	January 2002	February 2009	7	2.7	Yes	
F3a	FI	–	–	–	–	–	No	
F3b	FI	–	–	–	–	–	No	
F3c	FI	Initiation and stagnation	January 2006	March 2006	5	55	No	
		Propagation	September 2008	January 2009	10	66.7		
		Propagation and connect to F3a	June 2010	August 2010	7	75.2	No	Separation of iceberg January 2011
F4	FI	Propagation	January 2011	March 2011	0.5	5.5	No	
F5	FI	Propagation into crevasse prior to 2002	–	–	–	–	No	
F6	FI	–	–	–	–	–	No	
F7	FI	–	–	–	–	–	No	
				Filchner				
F1	FI	Propagation to front, iceberg calving	14 December 2004	28 December 2004	1	71	No	Exposed to calving front after calving of F3
F2	FI	Intersected by F3, iceberg calving	–	–	–	–	No	Served as calving boundary for F3
F3	FI	Propagation into F2, iceberg calving	November 2002	July 2003	11	57	No	
F4	FI	Propagation	November 2002	March 2012	7	2.1	No	
F5	FI	–	–	–	–	–	No	
F6	UPS (2)	–	–	–	–	–	–	
				Ronne				
R1	Wall	Propagation	October 2008	December 2009	6	14	No	Wintertime propagation
R2	FI–wall	Propagation	November 2002	December 2006	3	2.1	No	
R3	UPS (2)	–	–	–	–	–	No	
R4	UPS (2)	–	–	–	–	–	No	
R5	UPS (2)	–	–	–	–	–	No	
R6	FI	–	–	–	–	–	No	
R7	FI	Propagation	November 2002	March 2012	10	2.9	No	
				Larsen C				
LC1	Wall–FI	Propagation and iceberg calving	November 2002	January 2003	20	285	No	Calved iceberg January 2003
LC2	Wall–FI	Propagation, connect to crevasse and iceberg calving	January 2003	March 2005	21	27	No	Calved iceberg March 2005
		Propagation and iceberg calving	October 2005	March 2006	2	12.5	No	
LC3	Wall–FI	Propagation	March 2002	October 2007	3	1.5	No	
LC4	Wall	–	–	–	–	–	No	
LC5	Wall	–	–	–	–	–	No	
LC6	FI	Propagation	October 2005	January 2006	2.5	26	No	
		Propagation and iceberg calving	January 2009	February 2009	0.5	8.3	No	
LC7	FI	Propagation and iceberg calving (LC9)	13 December 2004	8 January 2005	16	550	No	
LC8	FI	–	–	–	–	–	No	
LC9	FI	Intersection by LC7 and iceberg calving	–	–	–	–	No	
LC10	FI	–	–	–	–	–	No	
LC11	UPS (2)	–	–	–	–	–	No	
LC12	Wall	–	–	–	–	–	No	

Table 1. (continued)

Name	Origin Location	Event Description	Start Date	End Date	Length Change (km)	Crevasse Rate (m/day)	Propagation Visible Field?	Notes
				Abbott				
A1	FI	Propagation and iceberg calving	17 February 2010	17 March 2010	2	66	No	
A2	FI	–	–	–	–	–	No	
A3	FI	Propagation and iceberg calving	14 October 2007	29 October 2007	1.5	100	No	
A4	FI	–	–	–	–	–	No	
A5	FI	Propagation and iceberg calving	2 January 2009	30 January 2009	1	36	No	
A6	FI filled	–	–	–	–	–	No	
A7	FI filled	–	–	–	–	–	No	
				Pine Island				
PIa	Wall	Propagation and iceberg calving	March 2007	October 2007		90	No	20×34 km^2
PIb	Wall	Propagation	October 2011	March 2013		40	No	
				Stange				
SS1	FI	–	–	–	–	–	No	
SS2	FI	–	–	–	–	–	No	
				Wilkins				
CI1	UPS (2)	Initiation parallel to CI2	May 2007	June 2007	20	550	No	Served as boundary for initial collapse in March 2008
CI2	UPS (2)	Stationary until served as collapse boundary	May 2008				No	Phase 2 of collapse
				George VI				
KG1	FI	–	–	–	–	–	No	Rift initiated directly opposing it, nascent iceberg 24×8 km^2
				Ross				
WR1	FI	Propagation and iceberg calving	June 2005	September 2005	2.5	27	No	Followed iceberg strike, resultant iceberg drifted away April 2006
WR2	UPS (2)	–	–	–	–	–	No	
WR3	UPS (2)	–	–	–	–	–	No	
WR4	UPS (2)	–	–	–	–	–	No	
WR5	UPS (2)	–	–	–	–	–	No	–
WR6	UPS (2)	Propagation	October 2003	March 2012	60 (total)	9.8 (total)	No	Wintertime propagation, propagation in both directions
Nascent	FI	Propagation	January 2002	November 2006	2	1.1	No	
ER8	UPS (2)	–	–	–	–	–	No	
ER9	UPS (2)	–	–	–	–	–	No	
ER10	UPS	–	–	–	–	–	No	
				Shackleton				
S1	FI	–	–	–	–	–	No	Pre-2002 iceberg remained in front
S2	FI	Propagation	November 2003	March 2008	4	2.4	No	Pre-2002 iceberg split, half moved away in 2003
				West				
BB1	FI	–	–	–	–	–	No	
BB2	FI	Split into TJ prior to 2002	–	–	–	–	No	
BB2a	TJ (BB2)	Propagation and iceberg calving	December 2004	January 2005	6	171	Yes	Iceberg drifted away by February 2005
BB2b	TJ	Propagation and crevasse intersection	September 2005	November 2005	0.5	2.7	Yes	
W3	FI	–	–	–	–	–	No	
W4	UPS (2)	–	–	–	–	–	Yes	
W5	UPS (2)	–	–	–	–	–	Yes	
W6	UPS (2)	–	–	–	–	–	Yes	
W7	UPS (2)	Propagation	January 2003	December 2009	20 (total)	7.9 (total)	Yes	Wintertime propagation

Table 1. (continued)

Name	Origin Location	Event Description	Start Date	End Date	Length Change (km)	Crevasse Rate (m/day)	Propagation Visible Field?	Notes
				Amery				
W1	FI	Initiation and propagation	October 2006	March 2012			No	
W2	FI	Propagation	January 2002	March 2012	No			
L1	FI	Split into TJ prior to 2002	–	–	–	–	No	
T1	TJ (L1)	Propagation	January 2002	March 2012			No	
T2	TJ (L1)	Propagation	January 2002	March 2012			No	
L2	FI	–	–	–	–	–	No	
E3	FI	Propagation	January 2002	March 2012			Yes	

[a]FI: front initiated; TJ: stem from triple junction; UPS (2): upstream double-ended rift; Wall: from margin.

3. Results

3.1. Patterns of Rift Behavior

[9] The observed rift activity types varied around the continent (Figure 2 and Table 1). These observations can be classified into two general behavioral categories, characterized by the recurrence interval between rift propagation events. These categories are (1) *dormant rifts*, defined as rifts that did not propagate over the decade (i.e., propagation is less than ∼500 m over the decade) and (2) *active rifts*, defined as rifts that lengthened by more than ∼500 m over the decade. Active rifts were further subdivided into (i) *continuously active rifts*, where the recurrence intervals between propagation events were comparable to or smaller than the repeat pass time of image acquisition, giving the appearance of continuous propagation; (ii) *intermittently active rifts*, which appeared to propagate continuously for 2 or more years before becoming dormant for the remainder of the decade; and (iii) *sudden burst active rifts*, which exhibited propagation events that were larger than ∼500 m after 2 or more years of dormancy.

[10] Of the 78 rifts monitored, 43 rifts (55%) showed no change in length and so qualified as dormant, making dormancy the primary behavior observed. Of the remaining 35 active rifts, seven were continuously active: five on the Amery Ice Shelf, one on the Fimbul Ice Shelf, and one on the Filchner Ice Shelf (supporting information Figures S1, S2, and S3). All seven of these rifts are front initiated. Another eight rifts were "intermittently active," propagating for at least 2 years before arresting. Of these eight intermittently active rifts, five were front initiated. Two more of these rifts were double-ended upstream rifts (one each on West Ice Shelf and on Ross Ice Shelf) that initiated in the interior of the ice shelf, away from the margins and lengthen from both rift tips (e.g., Figure S3, inset 2). The eighth intermittently active rift was in the remnant Larsen B Ice Shelf and initiated from the Jason Peninsula (Figure S5). The remaining 20 active rifts were sudden burst types.

3.2. Temporal Variation in Rift Propagation

[11] We examined temporal patterns in propagation for the 35 rifts that were active over some portion of the decade. Although there is a data gap during the Austral winter, for most rifts, the length of the rift at the end of each Austral summer was typically within one pixel of its length at the beginning of the following summer, indicating that rift propagation primarily occurs during the summer (Table 1), a finding consistent with *Fricker et al.* [2005]. There were three exceptions to this; we inferred wintertime propagation for one rift in the Ronne Ice Shelf, one in the West Ice Shelf, and one in the Ross Ice Shelf (Figure S12). The latter two rifts were both double-ended rifts that propagated from both ends.

[12] Temporal patterns of rift propagation were highly variable over the decade, ranging from 0 m day^{-1} up to 70 m days^{-1} within a single summer season, with little evidence of an Antarctic-wide change in rift propagation activity (Figure 3). However, we cannot rule out the possibility that variability over shorter time scales masks a longer-term secular change in rift propagation rates. Variability in propagation within a given ice shelf (and sometimes within a single rift) can be as large as the variability in rift propagation observed in different ice shelves. For example, rift propagation rates for different rifts in the Ross Ice Shelf varied between 0 and 50 m day^{-1}, similar to the range for all of the ice shelves; rift WR6 varied between 2 and 50 m day^{-1} over the decade (Figure S8).

4. Discussion

[13] The majority of rifts that we observed (43 of 78) were dormant for the entire decade. Many of these rifts initiated far upstream of the ice front and have been advecting downstream for decades with the main ice shelf flow [e.g., *Hulbe et al.*, 2010]. The fact that the majority of upstream rifts were dormant suggests that once these rifts become inactive, they are not easily reactivated. This is supported by observations of the crevasse field at the northeastern front of the Amery Ice Shelf (Figure S1). These crevasses advect toward the ice front but do not significantly change length once they have initiated upstream. In contrast, the most active rifts in our study were all front initiated, implying that iceberg calving may be more tightly controlled by near-calving front fracture processes than reactivation of dormant rifts that initiated upstream of the calving front.

[14] Previous studies have found conflicting evidence of whether rift propagation is driven by environmental variables (e.g., atmospheric temperatures and mechanical ocean forcing) or is limited by structural heterogeneity (e.g., marine ice formation and suture zones between ice streams). We used our decadelong data set to examine whether any of these hypotheses are consistent with the variability in

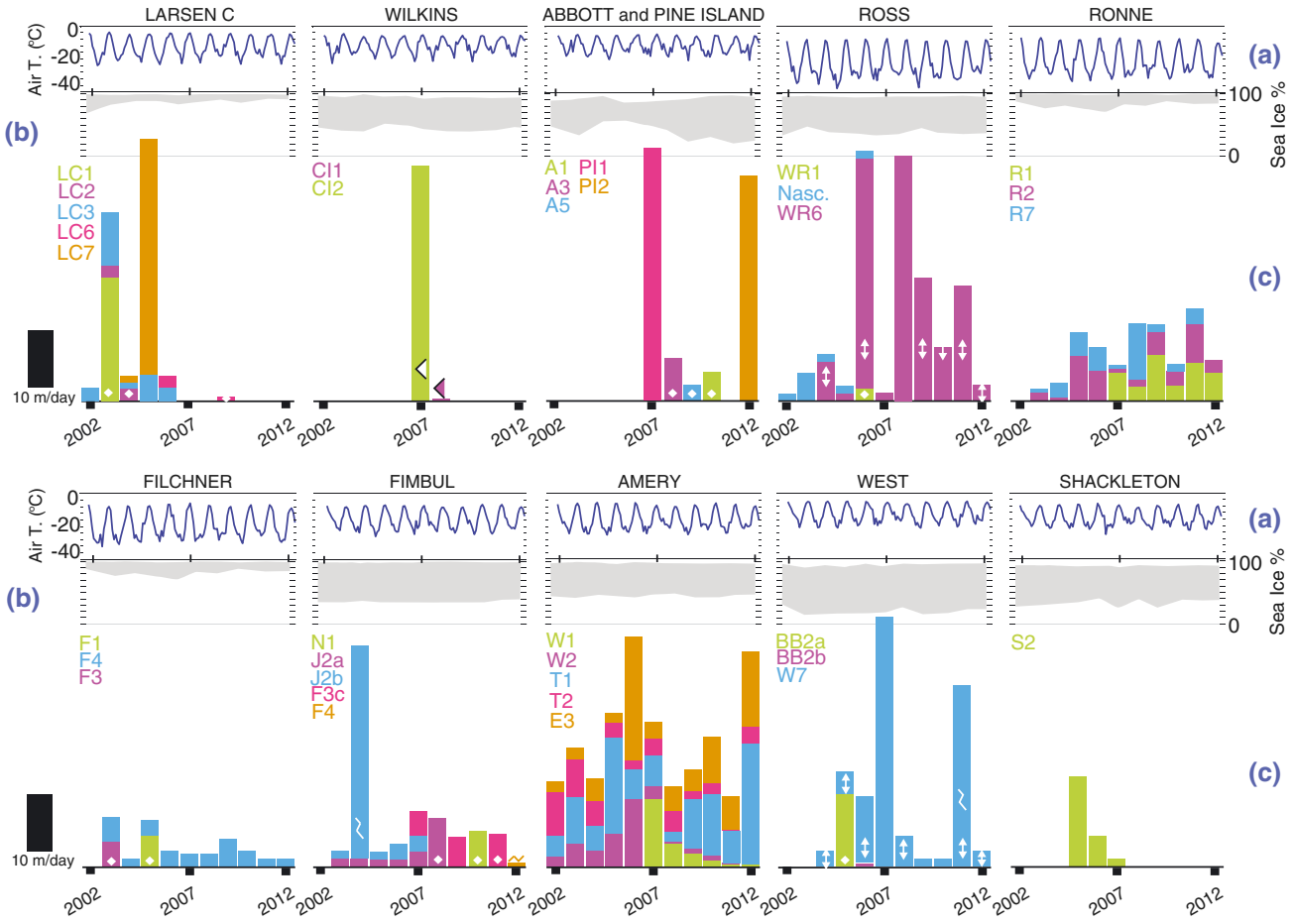

Figure 3. Atmospheric temperature, the monthly range of sea ice concentration from maxima and minima, and rift propagation rates for each ice shelf. (a and d) Monthly mean temperatures for each ice shelf over the decade, from ERA-Interim reanalysis data. (b and e) Gray-shaded regions are maximum and minimum annual sea ice extents in front of each ice shelf from passive microwave measurements. (c and f) The length of each bar represents the annual propagation rate with bars color coded to label the different rifts in ice shelves (Figures S1–S10). White arrows signify rifts with two actively propagating rift tips. White diamonds signify calving events. White zigzag signifies rifts propagating in a crevasse field. Left triangles signify a collapse event.

our observed propagation rates. Our observations do not exhibit a geographical trend that correlates with temperature differences around the continent, but we do observe that the location of rifts in an ice shelf affects the activity level of the rift. For example, *Humbert and Steinhage* [2011] showed that a small ice rumple changed the structure of the western section of Fimbul ice shelf rift area containing one of our active rifts—the only active rift in the western section of the shelf—between 2007 and 2012. Similarly, *Braun et al.* [2009] discussed the evolution of failure zones in the Wilkins Ice Shelf prior to several breakup events at ice rises within the ice. Below, we further examine possible controls on rift propagation.

4.1. Role of Environmental Forcing

4.1.1. Is Rift Propagation Triggered by Atmospheric Temperature?

[15] Previous studies have linked both warming atmospheric temperatures and mechanical forcing from the ocean to ice shelf disintegration [e.g., *Mueller et al.*, 2008]. This motivated us to test whether any of the variability in rift propagation regimes is correlated with atmospheric temperature fluctuation. For atmospheric temperature, we used monthly means of atmospheric reanalysis (ERA-Interim) 2 m air temperature data, at a spatial resolution of 1.5°, obtained from the European Centre for Medium-Range Weather Forecasts data server.

[16] Observed propagation rates displayed no obvious correlation with atmospheric temperature (Figure 3). Although warmer temperatures occur in more northern regions, rifts in those ice shelves (e.g., the Larsen C, Wilkins, and Abbott ice shelves) are no more active than those in colder ice shelves (e.g., the Ross and Filchner-Ronne ice shelves). For instance, similar to the ice shelves on the Antarctic Peninsula [e.g., *Barrand et al.*, 2013], the Shackleton Ice Shelf also exhibits surface melting during the summer months [*Ridley*, 1993]. While the Larsen C Ice Shelf contained five propagating rifts, the Shackleton Ice Shelf only has one active rift, S2, which only

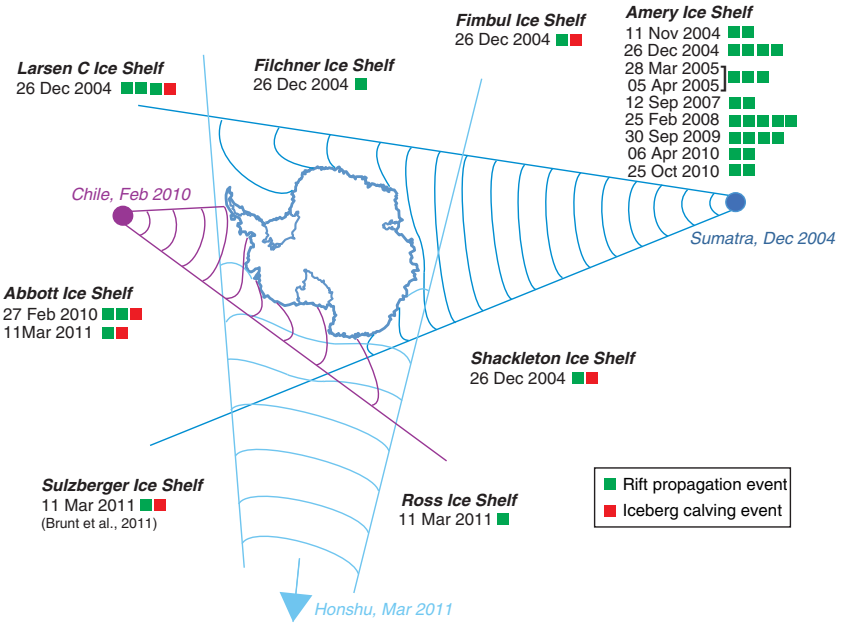

Figure 4. Examples of rifts that exhibited propagation events following the arrival of a tsunami. Each block indicates a rift that propagated following the arrival of a tsunami. The color of the block denotes whether the rift propagation event was also associated with an iceberg-calving event. Rift propagation was observed in the rifts that are exposed to the specific wave path of a given tsunami. Wave paths associated with tsunamis that originated near Sumatra, Chile, and Japan are sketched schematically from models of the relevant tsunami event (NOAA Center for Tsunami Research).

propagated for 2 years (2005–2007). We did not see a clear signal of an atmospheric temperature threshold, above which one or more rifts in a given ice shelf is prone to propagation. We found that above zero temperatures correlated with rift motion within 1 month only 20% of the time. In contrast, we found occasional correlations between summer rift activity and temperatures that were opposite to our expectations. For example, in winter 2007, the Amery, West, and Shackleton Ice Shelves experienced warmer-than-average winters, but active rifts in all three ice shelves showed a decreased propagation rate (the Amery and West Ice Shelves) or complete arrest (the Shackleton Ice Shelf) during the following Austral summer season. Similarly, three rifts in the Amery Ice Shelf (rifts W2, T1, and T2 in Figure S2) propagated over the wintertime in 2005, during a relatively cold winter when compared to average winter temperatures of other years.

4.1.2. Is Rift Propagation Triggered by Ocean Swell?

[17] Similar to the work of *Fricker et al.* [2005], we found seasonal variability in rift propagation rates (section 3.2) in which propagation rates during the summer were significantly higher than those in the winter period. *Fricker et al.* [2005] hypothesized that this could be explained by changes in oceanic circulation under the shelf, thawing and refreezing of ice mélange (dense pack of sea ice that fills in areas between rifts) or other factors that were as yet uncertain. Ice mélange was also hypothesized to have a stabilizing effect, for example, in the Ronne Ice Shelf [*Larour et al.*, 2004] and Jakobshavn in Greenland [*Amundson et al.*, 2010].

[18] To test the effects of mechanical forcing from the ocean, we analyzed changes in sea ice concentration over the range of ice shelves in our data set. We use sea ice as a proxy for mechanical ocean forcing because its presence will damp ocean waves [e.g., *Bassis et al.*, 2008]. The long wavelengths associated with infragravity waves [e.g., *Bromirski et al.*, 2010] will not be efficiently damped by sea ice, and their influence is not considered in this study. We retrieved monthly maxima and minima values of sea ice concentration relating to the area abutting the ice front to 5 km out to sea (Figure 3) from Nimbus-7 scanning multichannel microwave radiometer and Defense Meteorological Satellite Program special sensor microwave/imager special sensor microwave imager/sounder passive microwave data archived at the NSIDC. There is no correlation between sea ice concentration and rift activity on the decadal scale. For instance, the ice shelves that are adjacent to the Weddell Sea, e.g., the Larsen C, Ronne, and Filchner Ice Shelves, experience much less variability in sea ice concentration, since sea ice remains abundant throughout the year. However, these ice shelves do not exhibit decreased rift activity nor do we see evidence that an increase in rift activity is correlated with abnormally low sea ice concentration at any of the ice shelves. Using the monthly minima, we determined the months that showed minimum sea ice below the standard deviation (abnormally low concentration). We compared these lows with the rift data set to compute the correlation between a month with abnormally low sea ice concentration and rift propagation within the 1 month following. These events occurred together 12% of the time.

4.1.3. Is Ice Shelf Rift Propagation Triggered by Tsunamis?

[19] It has been previously suggested that the arrival of tsunamis may affect ice shelf rift propagation [e.g., *Brunt et al.*, 2011]. However, studies based on a single observed instance of a well-correlated propagation event

with a tsunami arrival are difficult to qualify as causal rather than it being simply coincidental [*Bassis et al.*, 2008]. Using our larger data set, we further investigated the likelihood that tsunamis might affect rift propagation. We did observe a correlation between the arrival of tsunamis and the propagation rifts, including some rifts that had previously been dormant. All five rifts in the Amery Ice Shelf propagated between 26 December 2004 and 9 January 2005, following the 26 December 2004 tsunami that originated west of Sumatra. Six additional incidences of rift propagation events on other ice shelves occurred at the end of December 2004. These ice shelves are all exposed to the Indian Ocean and were in line with computed wave paths and in situ buoy measurements, available from the National Oceanic and Atmospheric Administration (NOAA) Center for Tsunami Research. The only exception to this is the Ronne Ice Shelf, which did not experience any rift propagation events following the tsunami. Moreover, we observed additional instances of large rift propagation events in both the Amery Ice Shelf and other ice shelves following the arrival of other tsunamis originating in both the Indian and Pacific Oceans (Figure 4). "Large-propagation events" are defined here as events with a propagation rate above the interquartile range of the data. To determine if this connection is statistically significant or merely coincidence, we used a chi-square test [e.g., *Mighell*, 2000] to determine the probability that the coincidence between these events is random and found that the correlation between the arrival of the tsunami and the timing of large bursts of propagation is statistically significant at the 90% confidence level.

[20] Intriguingly, all of the instances in which we observed rift propagation following the arrival of a tsunami occurred in front-initiated rifts. These rifts are open to the ocean, and we hypothesize that fluctuations in wave height near the calving front can be channeled into the rift, and this wave field creates a large pressure concentration as the waves converge near the rift tip. A similar effect is observed in coastal regions where wave impacts cause cracks to propagate in near-shore rock cliffs [*Wolters and Muller*, 2001, 2004, 2008]. An order of magnitude estimate of the stress imparted to the crack tip shows that the pressure impulse can exceed 1 MPa even for modest changes in wave height, and this is sufficient to trigger full thickness failure of the ice [*Bassis and Walker*, 2011].

4.2. Role of Mechanical Forcing Controls on Rift Propagation

4.2.1. Suture Zones and Marine Ice

[21] We observed large variability in rift propagation in those rifts that were active but found little evidence that ice shelf-scale environmental forcing controls this variability. This led us to speculate that variability in rift propagation is controlled by mechanical heterogeneity, i.e., structural changes such as crevasses or changes in ice type and ice properties. It has been suggested previously that suture zones may serve as barriers to the propagation of rifts, as dormant rifts are often observed to coincide with suture zones between ice from adjacent ice streams [*Hulbe et al.*, 2010; *McGrath et al.*, 2012]. Table 1 shows that roughly one quarter of rifts that were dormant or intermittently active had propagated into a known suture zone in the shelf; however, this behavior is not universal. We observed at least two rifts propagate through nearby suture zones at an increased rate instead of arresting. For example, rift T1 in the Amery Ice Shelf (Figure S1) propagated through a suture zone. Rather than slowing down, it sped up as it propagated through the suture zone. Likewise, we observed rifts R1 and R2 on the Ronne Ice Shelf (Figure S4) propagate through suture zones prior to their arrest a year to 2 years later. *Jansen et al.* [2010] showed that suture zones have significant stabilizing effects on the Larsen C Ice Shelf. A comparison with their observations of Larsen C Ice Shelf shows that the dormant rifts observed in our study currently lie in regions with decreased stress intensity near the ice shelf front, whereas they likely initiated upstream in areas highlighted in the latter study as regions exceeding the critical stress intensity.

[22] Another possible factor in the variability in rift propagation may be the existence of marine ice, which may underlie suture zones and cause a variance in ice properties, leading to mechanical heterogeneity associated with different ice types within the ice shelf [e.g., *Fricker et al.*, 2001; *Craven et al.*, 2009; *Holland et al.*, 2010; *Jansen et al.*, 2010]. Unfortunately, we have insufficient observations of marine ice distributions at subkilometer scale to be able to more conclusively link observed variability in rift propagation rate to the presence of marine ice.

4.2.2. The Effect of Crevasses and Interaction Between Rifts

[23] We observed several large-propagation events that coincided with the intersection of a rift with a crevasse, suggesting that crevasses can serve as conduits for sudden bursts of rift propagation. Alternatively, crevasses that are not optimally oriented may instead hinder rift propagation. For example, when a rift intercepts a crevasse oriented perpendicular or at an angle to the rift, additional stress buildup may be required to either propagate along the nonoptimally oriented crevasse or for the rift to break through to the other side of the crevasse and continue propagating. However, once sufficient stress accumulates, the rift may propagate rapidly in a sudden burst and change direction. An example of this behavior occurs in rift E3 on the Amery Ice Shelf (Figure S1) where the rift propagates in a zigzag pattern, following the imprint of crevasses in the area. In total, 10 of the studied rifts were located in crevasse fields, and of these, only three were inactive (three on the West Ice Shelf, Figure S10). The observed influence of crevasses on rift propagation leads us to suggest that interaction between rifts and crevasses plays an important role in modulating likelihood of an episodic burst of propagation and controlling the average rift propagation rate. Although surface crevasses are most easily identified in satellite imagery, recent observations indicate that wide basal crevasses are often present within ice shelves and may also influence the propagation of ice shelf rifts but have subtle surface expressions not as readily apparent as surface crevasses in MODIS imagery [*McGrath et al.*, 2012].

5. Conclusions

[24] We have generated an observational record of Antarctic Ice Sheet-wide rift propagation over the decade 2002–2012, by observing rifts within 30 km of fronts on 13 Antarctic ice shelves. The variation in rifting behavior for the 78 rifts that we observed around the Antarctic Ice Sheet

emphasizes that rifting is a complex and variable process and reinforces that rift propagation is driven or controlled by more than one mechanism. Of the rifts we observed, we only found seven to be continuously active throughout the decade, all of which were front initiated. The remaining rifts fell into one of these categories: (i) completely dormant, without observable motion over the decade, (ii) sudden burst propagation in which large jumps in length occurred after years of dormancy, and (iii) intermittently active rift propagation for at least 2 years before arrest. We did not find an observable correlation between rifting activity and changes in local atmospheric temperatures or sea ice concentration. However, we found that the arrival of tsunamis may trigger rift propagation but only in those rifts that are front initiated. We believe this is because these types of rifts are open to the ocean, leading to enhanced mechanical interaction between the rift and the ocean. Our results suggest that rift propagation is complex but reinforces the hypothesis that mechanical heterogeneity within the ice shelf is an important control on rift propagation that needs to be further studied. Our data set represents the most geographically extensive record of rift propagation to date and provides a benchmark against which we can compare future rift activity.

[25] **Acknowledgments.** This work was supported by NASA grant NNX10AB216G, NSF CAREER-NSF-ANT 114085, and NSF grant EAGER-NSF-ARC 1064535. We would like to the thank the Editor Bryn Hubbard, the associate editor, and four reviewers whose comments substantially improved this manuscript.

References

Amundson, J. M., M. Fahnestock, M. Truffer, J. Brown, M. P. Luthi, and R. J. Motyka (2010), Ice mélange dynamics and implications for terminus stability, Jakobshavn Isbrae, Greenland, *J. Geophys. Res.*, *115*, F01005, doi:10.1029/2009JF001405.

Amundson, J. M., and M. Truffer (2010), A unifying framework for iceberg-calving models, *J. Glaciol.*, *56*, 822–830, doi:10.3189/002214310794457173.

Barrand, N. E., D. G. Vaughan, N. Steiner, M. Tedesco, P. Kuipers Munneke, M. R. Broeke, and J. S. Hosking (2013), Trends in Antarctic Peninsula surface melting conditions from observations and regional climate modeling, *J. Geophys. Res. Earth Surf.*, *118*, 315–330, doi:10.1029/2012JF002559.

Bassis, J. N., R. Coleman, H. A. Fricker, and J. B. Minster (2005), Episodic propagation of a rift on the Amery Ice Shelf, East Antarctica, *Geophys. Res. Lett.*, *320*, L06502, doi:10.1029/2004GL022048.

Bassis, J. N., H. A. Fricker, R. Coleman, and J.-B. Minster (2008), An investigation into the forces that drive ice-shelf rift propagation on the Amery Ice Shelf, East Antarctica, *J. Glaciol.*, *54*, 17–27, doi:10.3189/002214308784409116.

Bassis, J. N., and S. Jacobs (2013), Diverse calving patterns linked to glacier geometry, *Nat. Geosci.*, *6*, 833–836, doi:10.1038/ngeo1887.

Bassis, J. N., and C. C. Walker (2011), Upper and lower limits on the stability of calving glaciers from the yield strength envelope of ice, *Proc. Royal Soc. A*, *57*, 1–17, doi:10.1098/rspa.2011.0422.

Benn, D. I., C. R. Warren, and R. H. Mottram (2007), Calving processes and the dynamics of calving glaciers, *Earth Sci. Rev.*, *82*, 143–179, doi:10.1016/j.earscirev.2007.02.002.

Braun, M., A. Humbert, and A. Moll (2009), Changes of Wilkins Ice Shelf over the past 15 years and inferences on its stability, *Cryosphere*, *3*, 41–56.

Bromirski, P. D., O. V. Sergienko, and D. R. MacAyeal (2010), Transoceanic infragravity waves impacting Antarctic ice shelves, *Geophys. Res. Lett.*, *37*, L02502, doi:10.1029/2009GL041488.

Brunt, K. M., E. A. Okal, and D. R. Macayeal (2011), Antarctic ice-shelf calving triggered by the Honshu (Japan) earthquake and tsunami, March 2011, *J. Glaciol.*, *57*, 785–788, doi:10.3189/002214311798043681.

Craven, M., I. Allison, H. A. Fricker, and R. Warner (2009), Properties of a marine ice layer under the Amery Ice Shelf, East Antarctica, *J. Glaciol.*, *55*, 717–728, doi:10.3189/002214309789470941.

De Angelis, H., and P. Skvarca (2003), Glacier surge after ice shelf collapse, *Science*, *299*, 1560–1563, doi:10.1126/science.1077987.

Fahnestock, M. A., W. Abdalati, and C. A. Shuman (2002), Long melt seasons on ice shelves of the Antarctic Peninsula: An analysis using satellite-based microwave emission measurements, *Ann. Glaciol.*, *34*, 127–133, doi:10.3189/172756402781817798.

Fricker, H. A., S. Popov, I. Allison, and N. Young (2001), Distribution of marine ice beneath the Amery Ice Shelf, *Geophys. Res. Lett.*, *28*, 2241–2244, doi:10.1029/2000GL012461.

Fricker, H. A., N. W. Young, I. Allison, and R. Coleman (2002), Iceberg calving from the Amery Ice Shelf, East Antarctica, *Ann. Glaciol.*, *34*, 241–246, doi:10.3189/172756402781817581.

Fricker, H. A., N. W. Young, R. Coleman, J. N. Bassis, and J.-B. Minster (2005), Multi-year monitoring of rift propagation on the Amery Ice Shelf, East Antarctica, *Geophys. Res. Lett.*, *32*, L02502, doi:10.1029/2004GL021036.

Glasser, N. F., B. Kulessa, A. Luckman, D. Jansen, E. C. King, P. R. Sammonds, T. A. Scambos, and K. C. Jezek (2009), Surface structure and stability of the Larsen C ice shelf, Antarctic Peninsula, *J. Glaciol.*, *55*, 400–410, doi:10.3189/002214309788816597.

Holdsworth, G. (1974), Erebus Glacier tongue, McMurdo Sound, Antarctica, *J. Glac.*, *13*, 27–35.

Holdsworth, G. (1977), Tidal interaction with ice shelves, *Ann. Geophys.*, *33*, 133–146.

Holland, P., H. Corr, D. Vaughan, A. Jenkins, and P. Skvarca (2010), Marine ice in the Larsen Ice Shelf, *Geophys. Res. Lett.*, *36*, L11604, doi:10.1029/2009GL038162.

Hulbe, C. L., C. Ledoux, and K. Cruikshank (2010), Propagation of long fractures in the Ronne Ice Shelf, Antarctica, investigated using a numerical model of fracture propagation, *J. Glaciol.*, *56*, 459–472, doi:10.3189/002214310792447743.

Humbert, A., and D. Steinhage (2011), The evolution of the western rift area of the Fimbul Ice Shelf, Antarctica, *The Cryosphere Discuss.*, *5*, 1089–1122, doi:10.5194/tcd-5-1089-2011.

Jacobs, S. S., D. R. MacAyeal, and J. L. Ardai Jr. (1986), The recent advance of the Ross Ice Shelf, Antarctica, *J. Glaciol.*, *32*, 464–474.

Jansen, D., B. Kulessa, P. R. Sammonds, A. Luckman, E. C. King, and N. F. Glasser (2010), Present stability of the Larsen C ice shelf, Antarctic Peninsula, *J. Glaciol.*, *56*, 593–600, doi:10.3189/002214310793146223.

Jansen, D., A. Luckman, B. Kulessa, P. R. Holland, and E. C. King (2013), Marine ice formation in a suture zone on the Larsen C Ice Shelf and its influence on ice shelf dynamics, *J. Geophys. Res. Earth Surf.*, *118*, 1628–1640, doi:10.1002/jgrf.20120.

Joughin, I., and D. R. MacAyeal (2005), Calving of large tabular icebergs from ice shelf rift systems, *Geophys. Res. Lett.*, *32*, L02501, doi:10.1029/2004GL020978.

Joughin, I., R. B. Alley, and D. M. Holland (2012), Ice-sheet response to oceanic forcing, *Science*, *338*, 1172–1176, doi:10.1126/science.1226481.

Larour, E., E. Rignot, and D. Aubry (2004), Modelling of rift propagation on Ronne Ice Shelf, Antarctica, and sensitivity to climate change, *Geophys. Res. Lett.*, *31*, L16404, doi:10.1029/2004GL020077.

Lazzara, M. A., K. C. Jezek, T. A. Scambos, D. R. MacAyeal, and C. J. van der Veen (1999), On the recent calving of icebergs from the Ross Ice Shelf, *Polar Geogr.*, *23*, 201–212, doi:10.1016/j.icarus.2007.07.016.

Legresy, B., A. Wendt, I. Tabacco, F. Remy, and R. Dietrich (2004), Influence of tides and tidal current on Mertz Glacier, Antarctica, *J. Glaciol.*, *50*, 427–435, doi:10.3189/172756504781829828.

Lescarmontier, L., B. Legresy, R. Coleman, F. Perosanz, C. Mayet, and L. Testut (2012), Vibrations of Mertz Glacier ice tongue, East Antarctica, *J. Glaciol.*, *58*, 665–676, doi:10.3189/2012JoG11J089.

Luckman, A., D. Jansen, B. Kulessa, E. C. King, P. Sammonds, and D. I. Benn (2012), Basal crevasses in Larsen C Ice Shelf and implications for their global abundance, *The Cryosphere*, *6*, 113–123, doi:10.5194/tc-6-113-2012.

MacAyeal, D. R., et al. (2006), Transoceanic wave propagation links iceberg calving margins of Antarctica with storms in tropics and Northern Hemisphere, *Geophys. Res. Lett.*, *33*, L17502, doi:10.1029/2006GL027235.

McGrath, D., K. Steffen, H. Rajaram, T. Scambos, W. Abdalati, and E. Rignot (2012), Basal crevasses on the Larsen C Ice Shelf, Antarctica: Implications for meltwater ponding and hydrofracture, *Geophys. Res. Lett.*, *39*, L16504, doi:10.1029/2012GL052413.

Mighell, K. (2000), Goodness-of-fit testing of low-count data using the modified chi-square-gamma statistic, paper presented at American Astronomical Society Meeting Abstracts, Bulletin of the American Astronomical Society, vol. 32, p. 762.

Mueller, D. R., L. Copland, A. Hamilton, and D. Stern (2008), Examining Arctic ice shelves prior to the 2008 breakup, *EOS Transactions*, *89*, 502–503, doi:10.1029/2008EO490002.

Pritchard, H. D., S. R. M. Ligtenberg, H. A. Fricker, D. G. Vaughan, M. R. van den Broeke, and L. Padman (2012), Antarctic ice-sheet loss driven by basal melting of ice shelves, *Nature*, *484*, 502–505, doi:10.1038/nature10968.

Rack, W., and H. Rott (2004), Pattern of retreat and disintegration of Larsen B Ice Shelf, Antarctic Peninsula, *Ann. Glaciol.*, *39*, 505–510, doi:10.3189/172756404781814005.

Ridley, J. (1993), Surface melting on Antarctic Peninsula ice shelves detected by passive microwave sensors, *Geo. Res. Lett.*, *20*, 2639–2642, doi:10.1029/93GL02611.

Rignot, E., G. Casassa, P. Gogineni, W. Krabill, A. Rivera, and R. Thomas (2004), Accelerated ice discharge from the Antarctic Peninsula following the collapse of Larsen B Ice Shelf, *Geophys. Res. Lett.*, *31*, L18401, doi:10.1029/2004GL020697.

Rignot, E., J. L. Bamber, M. R. van den Broeke, C. Davis, Y. Li, W. J. van de Berg, and E. van Meijgaard (2008), Recent Antarctic ice mass loss from radar interferometry and regional climate modelling, *Nat. Geosci.*, *1*, 106–110, doi:10.1038/ngeo102.

Rignot, E., S. Jacobs, J. Mouginot, and B. Scheuchl (2013), Ice-Shelf Melting Around Antarctica, *Science*, *341*, 266–270, doi:10.1126/science.1235798.

Robinson, W., and T. G. Haskell (1990), Calving of Erebus Glacier tongue, *Nature*, *346*, 615–616, doi:10.1038/346615b0.

Rott, H., P. Skvarca, and T. Nagler (1996), Rapid collapse of Northern Larsen ice shelf, Antarctica, *Science*, *271*, 788–792, doi:10.1126/science.271.5250.788.

Rott, H., W. Rack, T. Nagler, and P. Skvarca (1998), Climatically induced retreat and collapse of northern Larsen Ice Shelf, Antarctic Peninsula, *Ann. Glaciol.*, *27*, 86–92.

Rott, H., W. Rack, P. Skvarca, and H. de Angelis (2002), Northern Larsen Ice Shelf, Antarctica: Further retreat after collapse, *Ann. Glaciol.*, *34*, 277–282, doi:10.3189/172756402781817716.

Scambos, T. A., J. Bohlander, and B. Raup (1996), *Images of Antarctic Ice Shelves. [2002–2012]*, National Snow and Ice Data Center, Boulder, Colorado, USA.

Scambos, T. A., C. Hulbe, M. Fahnestock, and J. Bohlander (2000), The link between climate warming and break-up of ice shelves in the Antarctic Peninsula, *J. Glaciol.*, *46*, 516–530, doi:10.3189/172756500781833043.

Scambos, T. A., C. Hulbe, and M. Fahnestock (2003), Climate-induced ice shelf disintegration in the Antarctic Peninsula, *Antarct. Res. Ser.*, *79*, 79–92, doi:10.1029/AR079p0079.

Scambos, T. A., J. A. Bohlander, C. A. Shuman, and P. Skvarca (2004), Glacier acceleration and thinning after ice shelf collapse in the Larsen B embayment, Antarctica, *Geophys. Res. Lett.*, *31*, L18402, doi:10.1029/2004GL020670.

Sergienko, O. V. (2010), Elastic response of floating glacier ice to impact of long-period ocean waves, *J. Geophys. Res.*, *115*, F04028, doi:10.1029/2010JF001721.

Steffen, K., P. U. Clark, J. G. Cogley, D. Holland, S. Marshall, E. Rignot, and R. Thomas (2008), Rapid changes in glaciers and ice sheets and their impacts on sea level, in *Abrupt Climate Change*, pp. 60–142, A Report by the U.S. Climate Change Science Program and the Subcommittee on Global Change Research, U.S. Geological Survey, Reston, VA.

Vaughan, D. G., and C. S. M. Doake (1996), Recent atmospheric warming and retreat of ice shelves on the Antarctic Peninsula, *Nature*, *379*, 328–331, doi:10.1038/379328a0.

Wolters, G., and G. Muller (2001), The effect of wave action on structures with large cracks, paper presented Ocean Wave Measurement and Analysis: Proceedings of the Fourth Int. Symposium: WAVES 2001. 4th International Symposium of Ocean Wave Measurement and Analysis: WAVES 2001, American Society of Civil Engineers, 1773–1782.

Wolters, G., and G. Muller (2004), The Propagation of Wave Impact Induced Pressures Punto Cracks and Fissures, in *Coastal Chalk Cliff Instability*, pp. 121–130, Geological Society London Engineering Geology, Geological Society London, doi:10.1144/GSL.ENG.2004.020.01.09.

Wolters, G., and G. Muller (2008), Effect of cliff shape on internal stresses and rock slope stability, *J. Coastal Res.*, *24*, 43–50, doi:10.2112/05-0569.1.